Journal of Luminescence 210 (2019) 58–65

Contents lists available at ScienceDirect

Journal of Luminescence

journal homepage: www.elsevier.com/locate/jlumin

Dosimetric and optical properties of $CaSO_4$:Tm and $CaSO_4$:Tm,Ag crystals produced by a slow evaporation route

Danilo O. Junot[a,b,*], Ana G.M. Santos[a], Patrícia L. Antonio[b], Marcos V.S. Rezende[a], Divanizia N. Souza[a], Linda V.E. Caldas[b]

[a] Departamento de Física, Universidade Federal de Sergipe, São Cristóvão, SE, Brazil
[b] Instituto de Pesquisas Energéticas e Nucleares/Comissão Nacional de Energia Nuclear, São Paulo, Brazil

ARTICLE INFO

Keywords:
Dosimetry
Thermoluminescence
$CaSO_4$

ABSTRACT

The motivation of this work was to produce TL dosimeters based on crystals of $CaSO_4$ doped with thulium and silver, by means of a suitable new route. The crystals were produced by an adaptation of the slow evaporation route using calcium carbonate ($CaCO_3$) as precursor, and incorporating the dopants (Tm_2O_3 and silver nanoparticles) in a solution of sulfuric acid, which is evaporated resulting in $CaSO_4$:Tm or $CaSO_4$:Tm,Ag crystal powders. X-ray diffraction analyses showed that the produced samples exhibit only a single phase corresponding to the crystal structure of anhydrite. Optical characterization was performed to determine the band gap of the materials. Samples did not show a reasonable OSL signal after stimulation with blue LEDs. TL characteristics such as glow curves, linearity and reproducibility of response, minimum detectable dose and fading were evaluated. The $CaSO_4$:Tm samples showed TL emission glow curves with peaks in temperatures proper for dosimetry. The $CaSO_4$:Tm,Ag samples presented a very intense peak displaced to high temperatures that could only be observed by applying heating rates below 4 °C/s. Samples doped with thulium oxide and silver nanoparticles showed the highest TL intensity and lowest fading.

1. Introduction

The widespread use of ionizing radiation in medicine and industry, associated with the known risks that this type of radiation can cause, has motivated the search for new radiation detectors. The themoluminescence (TL) technique has been used for this application since the decade of 1940 and different materials have been proposed as dosimeters [1].

Optically stimulated luminescent (OSL) dosimeters, although more recently than thermoluminescent dosimeters, are already well established in personal dosimetry, being used commercially for more than a decade. This type of dosimetry became attractive due to its fast reading without heating and the possibility of re-reading to confirm the estimation of absorbed doses [2].

Several $CaSO_4$ based materials are already well known and widely used in dosimetric applications. $CaSO_4$:Dy, also known as TLD-900, has become one of the most common TL dosimeters due to its high sensitivity, low minimum detectable dose, wide range of linearity and high saturation level [1]. However, it is important to further research on addition of new doping elements to the sulfate matrix, in order to improve the luminescent response of such material. It is also important to advance research seeking new viable production routes with sensitive dosimeters at low cost.

Therefore, Madhusoodanan et al. [3] reported that in addition to rare-earth (RE) elements, Ag particles improve the luminescent characteristics of $CaSO_4$, and they shift its major TL peak from 200 °C to ~ 400 °C, without changes in the photoluminescence (PL) emission. Kulkarni et al. [4] and Guckan et al. [5] reported the applicability of $CaSO_4$:Eu for OSL dosimetry. Kearfott et al. [6] also reported a possible application of $CaSO_4$:Tm in OSL dosimetry. However, there are no reports on the use of $CaSO_4$:Tm,Ag in this type of dosimetry. In recent years, there has been much research involving luminescent materials on a nanometric scale [7–10]. Yashaswini et al. [11] evaluated the photoluminescence of $CaSO_4$ nanoparticles, but did not explain the physical phenomena related to the reduced size of the particle. Junot et al. [12] observed that the incorporation of silver in $CaSO_4$:Eu allows more intense TL and thermally stimulated exoelectronic emissions (TSEE) than in materials without silver. The increase in the emission intensity has shown to be more significant when silver is incorporated as a co-dopant in the form of nanoparticles [13,14]. However, the energy transfer

* Corresponding author.
E-mail address: dan.junot@gmail.com (D.O. Junot).

https://doi.org/10.1016/j.jlumin.2019.02.005
Received 19 July 2018; Received in revised form 22 November 2018; Accepted 3 February 2019
Available online 05 February 2019

mechanisms of silver nanoparticles in the crystalline lattice of $CaSO_4$:RE are still unknown.

The main goal of this work was to evaluate the dosimetric properties of $CaSO_4$,Tm and $CaSO_4$:Tm,Ag produced by the new method proposed by Junot et al. [15]. $CaSO_4$:Tm is a very popular dosimetric $CaSO_4$ based material, mostly because of its high sensitivity and proper dosimetric peak temperature (230 °C) [16,17], and this material co-doped with silver nanoparticles has never been investigated. The TL of the samples was studied with the objective of evaluating their applicability for dosimetry, considering characteristics such as sensitivity, dose response, linearity, reproducibility, minimum detectable dose and fading.

2. Materials and methods

The samples were produced by the means of the following steps:

1. The silver particles synthesis was performed by the poliol method applied by Junot et al. [13]. This method is based on reducing the silver of the precursor agent $AgNO_3$ (Neon 99%) in ethylene glycol. Addition of the reducing agent $NaBH_4$ (Vetec 98%) is performed slowly with the aid of a syringe. The solution is kept in an ice bath under vigorous magnetic stirring, otherwise the silver particles undergo strong agglomeration. The silver is separated from the reaction medium by centrifugation, washed three times with isopropyl alcohol and dried at a temperature of 80 °C.
2. Calcium carbonate ($CaCO_3$) (J.T. Baker 99%), thulium oxide (Tm_2O_3) (Sigma-Aldrich 99.9%) and silver particles were dissolved in a solution of sulfuric acid (H_2SO_4) (Vetec 95–99%), that is evaporated leaving just $CaSO_4$:Tm or $CaSO_4$:Tm,Ag crystal powder. Details of the crystal growth route are described in Junot et al. [15]. The Tm^{3+} and Ag ions were incorporated in a ratio of 1:1, at 0.1% mol concentration.
3. The pellets with 6 mm diameter, 1 mm thickness, and 40 mg mass were obtained using a 1:1 (weight) mixture of the phosphor and Teflon, to improve physical resistance, and sintered at 400 °C for 1 h.

The samples were irradiated with a beta radiation source ($^{90}Sr/^{90}Y$ from Risö TL/OSL reader, at a rate of 0.1 Gy/s) at a dose range from 0.1 Gy to 10 Gy.

With the purpose to confirm the crystalline structure present in the samples, X-ray diffraction data (XRD) were obtained in a Rigaku diffractometer of Bragg-Brentano geometry using Cu-Kα radiation. The measurements were performed in the continuous mode with a scan range of 20–80°, scan step of 0.02 and scan speed of 2°/min.

The optical characterization of the samples was carried out at the Brazilian Synchrotron Light Laboratory (LNLS) using the facilities of the Toroidal Grating Monochromator (TGM) beamline. The TGM beamline provides photons with energies ranging from 12 eV to 330 eV (flux up to 10^{13} photons/s, resolving power up to 700) [18]. The measurements were performed at room temperature and at ultra-high vacuum conditions using the standard sample chamber available in the TGM beamline, with some additions like an optical fiber, photomultiplier tube and housing, spectrometers and monochromator for the range 200–1000 nm. An excitation range from 4.5 eV to 10 eV was utilized by applying filters of quartz and MgF_2, with steps of 0.5 eV.

TL analyses were performed in a Risö TL/OSL reader using different heating rates in the range from 1 °C/s to 10 °C/s, to a maximum temperature of 400 °C. In order to carry out measurements of the TL emission spectra, a high resolution spectrometer from Ocean Optics was coupled in place of the photomultiplier. OSL measurements were also carried out in the Risö TL/OSL reader. For the excitation of the samples, blue LEDs (Light Emitting Diodes), with emission at 470 nm, and continuous-wave mode were used. The signal was collected over 40 s. All pellets were protected against light exposure during irradiation (inside the reader), and they were exposed to radiation and evaluated at the same side surface. Before every measurement, a background reading was performed, recorded and subtracted from the current reading to avoid any interference from the background light and the equipment infrared (IR) emission.

To study the TL response reproducibility of the composites, 50 pellets from each material were produced, each of them with a mass of 40 mg. The pellets were irradiated with 1 Gy ($^{90}Sr/^{90}Y$), evaluated at the TL reader at a heating rate of 10 °C/s, thermally treated and irradiated again, creating a cycle, which was carried out 5 times. After each irradiation-readout cycle, the pellets were treated thermally during 1 h at 400 °C. After the OSL measurements, the samples were treated optically during 1 h inside a box with white LEDs with a total illuminance of 22.000 lx.

To study the fading, TL analyses were carried out immediately after irradiation and after one day, 7 days, 15 days and 30 days. During the time interval between irradiation and reading, all of the samples were stored in an opaque packaging at room temperature (approximately 23 °C), and under low light conditions.

In order to minimize the uncertainties, all results in this work represent the average of at least three different measurements.

3. Results and discussion

3.1. Crystalline Structure

Fig. 1 presents the results from XRD for samples of pure $CaSO_4$ (JT Baker 99%) and samples of $CaSO_4$:Tm, and $CaSO_4$:Tm,Ag prepared in powder form, after calcination. The diffraction patterns obtained for all samples presented diffraction peaks and relative intensities corresponding to the structure of anhydrite (JCPSD 01-072-0916). Thus, it can be seen that the samples of pure and doped $CaSO_4$ showed only a single phase, which was expected since it is not possible to observe the presence of dopants due to their low concentrations (0.1% mol). These results confirm that the samples are composed of crystals with orthorhombic symmetry and spatial group Amma.

3.2. Optical emission/excitation

The Visible/Ultraviolet (VUV) emission and excitation spectra of $CaSO_4$:Tm and $CaSO_4$:Tm,Ag samples using synchrotron radiation are displayed in Figs. 2 and 3. The emission spectra under 166 nm (7.45 eV) excitation exhibit similar features, except by the intensity difference, with either peaks with maxima at about 342 nm ($^3P_0 \rightarrow {}^3H_4$), 360 nm ($^1D_2 \rightarrow {}^3H_6$), 455 nm ($^1D_2 \rightarrow {}^3H_4$), 480 nm ($^1G_4 \rightarrow {}^3H_6$), 515 nm ($^1D_2 \rightarrow {}^3H_5$), 660 nm ($^3F_{2,3} \rightarrow {}^3H_6$), 750 nm ($^3P_0 \rightarrow {}^1G_4$) and 788 nm ($^3H_4 \rightarrow$

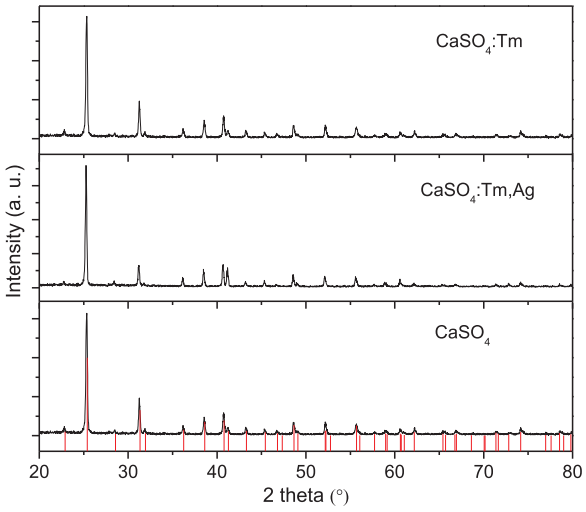

Fig. 1. X-ray diffraction of crystalline samples of $CaSO_4$, $CaSO_4$:Tm and $CaSO_4$:Tm,Ag.

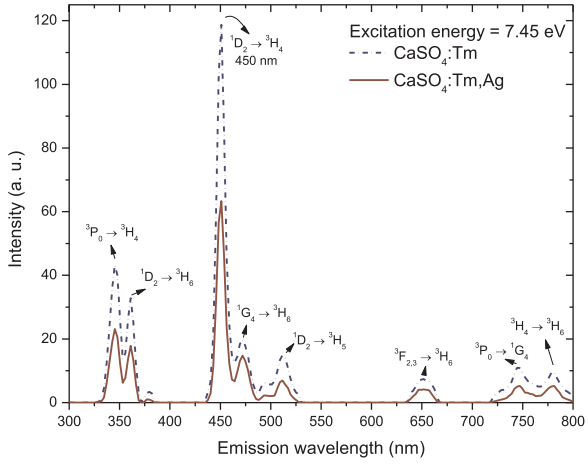

Fig. 2. Emission spectra of $CaSO_4$:Tm and $CaSO_4$:Tm,Ag samples.

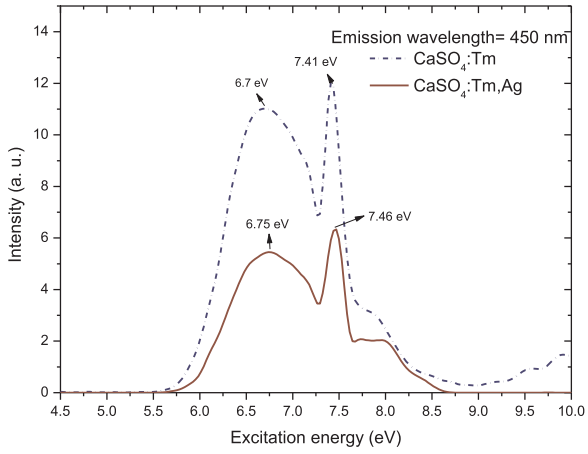

Fig. 3. Excitation spectra of $CaSO_4$:Tm and $CaSO_4$:Tm,Ag samples.

$^3H_6$), corresponding to the Tm^{3+} ion transitions [19]. It can be noted that the presence of Ag codopant contributes to a decrease on the emission intensity. The excitation spectrum (Fig. 3) of 450 nm emission exhibits two strong broad bands and a weak band. Again, excitation spectra exhibit similar features, except by the intensity difference. The band peaking at around 8.2 eV (151 nm) is assigned to the host lattice absorption from the top of the valence band (VB) to the bottom of the conduction band (CB), *i.e.* the host band gap (E_g). This band gap energy (E_g) can be estimated using the minimum of the first derivative of the excitation spectra. This value is considerably lower than that obtained from density functional theory (DFT) calculations and the results of the spectroscopy measurements [20]. The comparison with literature band gap values from other orthosulphates [21,22] indicates that the value close to 9 eV is reasonable for orthosulphates. It is also possible to note that the silver particles do not change the band gap of the $CaSO_4$ material. The second and third bands, with maxima at 6.70 eV (185 nm) and 7.41 eV (167 nm), are associated to the band position of 4f-5d transition and $O^{2-} \rightarrow Tm^{3+}$ charge transfer excitation of Tm^{3+} ions, respectively. The difference on the emission and excitation spectra caused by the Ag codopant is probably attributed to the change in the Tm local symmetry. Upon codoping an Ag^+ ion, local charge compensation may occur in which one Ag^+ replaces one Ca^{2+} or S^{4+} host site. This would lead to a decrease on the site symmetry for Tm^{3+} ion. 3D spectra of $CaSO_4$:Tm and $CaSO_4$:Tm,Ag samples are shown in Figs. 4 and 5, respectively.

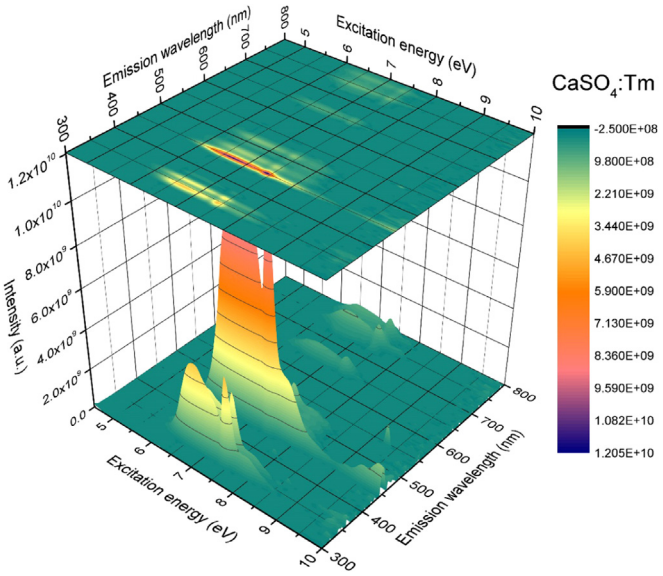

Fig. 4. 3D Emission/excitation spectra of $CaSO_4$:Tm samples.

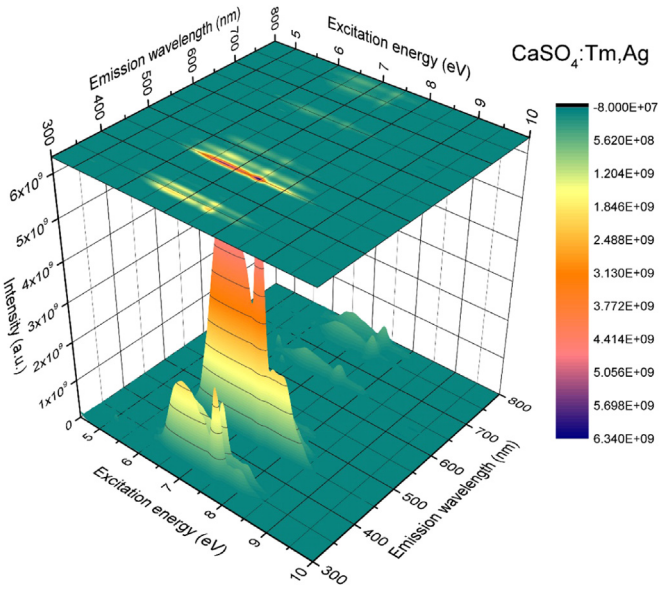

Fig. 5. 3D Emission/excitation spectra of $CaSO_4$:Tm,Ag samples.

3.3. Glow curves

Fig. 6a shows a comparison of the glow curves of the two samples produced, after absorbed doses of 100 mGy ($^{90}Sr/^{90}Y$) using a heating rate of 10 °C/s in the reader. The presence of three main peaks can be observed in the TL emission curve of each material. $CaSO_4$:Tm presents peaks at temperatures of 145 °C, 200 °C and 300 °C. $CaSO_4$:Tm,Ag exhibits peaks at temperatures of 180 °C, 270 °C and 340 °C. As the melting point of Teflon, a constituent of the pellets, is around 400 °C [23], the pellets were read at a heating rate of 1 °C/s in order to study the peak at high temperature in the TL signal of the $CaSO_4$:Tm,Ag samples. Fig. 6b shows a comparison of the emission curves of the $CaSO_4$:Tm and $CaSO_4$:Tm,Ag samples after absorbed doses of 100 mGy ($^{90}Sr/^{90}Y$), using a heating rate of 1 °C/s in the reader. With the lower heating rate, there is a displacement of approximately 70 °C in both TL curves, so that it is possible to observe the signal of the main peak of the $CaSO_4$:Tm,Ag samples at 380 °C. As already observed by Madhusoodanan et al. [24], the Ag presence shifts the 230 °C peak to 380 °C, but with comparable intensities. The key point here is that the presence of

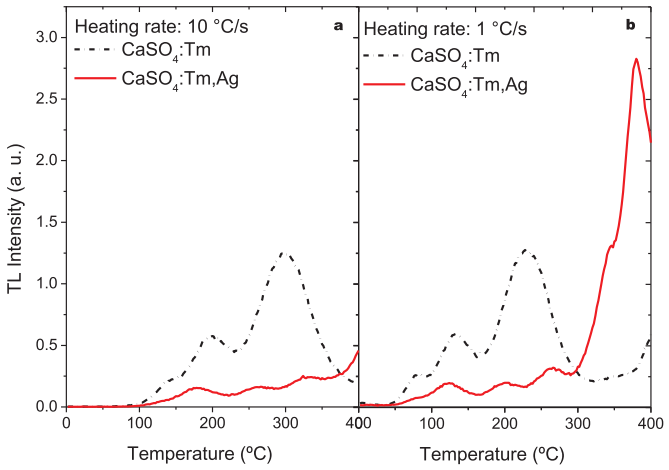

Fig. 6. Typical TL glow curves of $CaSO_4$:Tm and $CaSO_4$:Tm,Ag samples after absorbed doses of 100 mGy from a ^{90}Sr /^{90}Y source, evaluated at heating rates of 10 °C/s (a) and 1 °C/s (b).

silver particles in nanoscale enhances the TL emission intensity by a factor of approximately 3. The poliol method employed in the silver particles synthesis is a well know production route to obtain particles with size in nanoscale. In this method, the formation of silver nanoparticles can be confirmed by the change in the coloration of the colorless silver nitrate solution to amber yellow [25], as observed in the synthesis. In a previous study of the group [13] it was observed that samples of powdered $CaSO_4$:Eu,Ag show a considerably more intense emission (approximately 5 times greater) than the samples containing only europium or silver as dopants. This was also observed in this study for the samples with thulium, and that fact suggests that silver nanoparticles may be altering the crystal lattice of the material, creating new defects and traps for electrons. Besides that, in nanocrystalline materials the percentage of surface defects, such as incomplete valence atoms, stacking faults or grain boundary, are relatively high in comparison to bulk crystalline materials [26]. It is important to notice that, considering the integral below the curve, the sensitivity of $CaSO_4$:Tm,Ag is higher than the sensitivity of $CaSO_4$:Tm only for low heating rates. For standard measurements (with the heating rate of 10 °C/s), $CaSO_4$:Tm presents a slightly higher sensitivity.

In order to better evaluate the effect of the heating rate on the TL signal of the samples, TL readings of the samples produced were performed by varying the heating rate from 1 °C/s to 10 °C/s in steps of 1 °C/s. The results are shown in Fig. 7 for $CaSO_4$:Tm and in Fig. 8 for $CaSO_4$:Tm,Ag. The inset graphs show the TL response (total area under

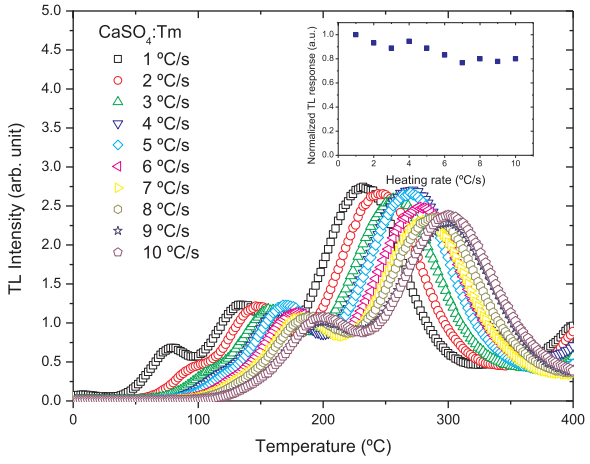

Fig. 7. TL glow curves of $CaSO_4$:Tm samples as a function of heating rate after irradiation of 100 mGy (^{90}Sr/^{90}Y).

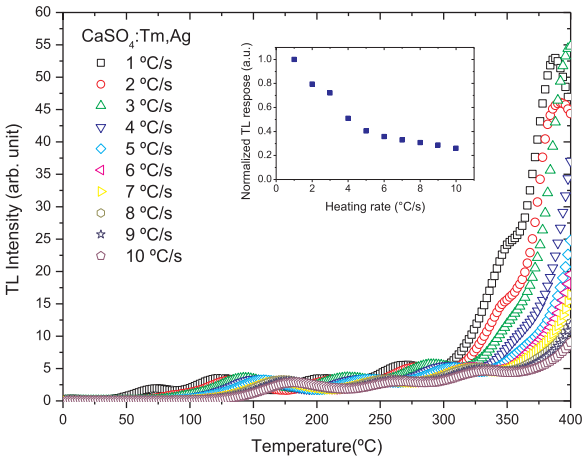

Fig. 8. TL glow curves of $CaSO_4$:Tm,Ag samples as a function of heating rate after irradiation of 100 mGy (^{90}Sr/^{90}Y).

the curve) as a function of the heating rate. It is possible to observe that, for both samples, there was an average displacement (for lower temperatures) of 7 °C in the peak temperatures for each increase of 1 °C/s in the heating rate. This is an expected result, since the probability of the electrons escaping their traps changes with the heating rate variation. In standard dosimetry, usually a heating rate of 10 °C/s is used. However, varying the heating rate it is possible to evaluate some effects, such as the thermal quenching effect. It can be defined as the reduction of the intensity of the TL signal with the increase of the heating rate [27]. If the area below the glow curve remains constant regardless of the heating rate, there is no thermal quenching effect, what was observed for all studied samples. As the TL signal of the $CaSO_4$:Tm samples does not present peaks at elevated temperatures (above 400 °C), there is little dependence on the TL response with the variation of the heating rate. However, the TL signal of the $CaSO_4$:Tm,Ag samples is strongly influenced by the heating rate, once, at rates above 4 °C/s, the intense peak at elevated temperatures is no longer observed, resulting in an approximately 70% reduction in the TL response of these materials. It is possible to notice that this reduction in the TL response is solely due to a high intensity peak in a critical temperature, and must not be interpreted as a thermal quenching effect.

For the assessment of the peaks composing the TL emission curves of the produced samples, the (T_m-T_{stop}) technique was applied to these samples. This technique consists of heating the sample to a given temperature called T_{stop} and evaluating the average temperature of the lowest temperature peak observed (T_m). The samples were irradiated with 100 mGy and the initial T_{stop} temperature for partially heating was 100 °C. After this, the sample was cooled and the complete glow curve was obtained in order to extract the T_m value. The T_{stop} temperature was varied in increments of 5 °C and the final T_{stop} temperature was 320 °C. With the data obtained, the graph "T_m x T_{stop}" was plotted, as shown in Fig. 9, for the $CaSO_4$:Tm and $CaSO_4$:Tm,Ag samples. The dashed lines represent the temperatures of the TL peaks observed in the TL curve of the samples. The presence of three peaks can be verified at temperatures of 190 °C, 270 °C and 340 °C, for samples of $CaSO_4$:Tm,Ag, and two peaks at temperatures of 200 °C and 300 °C, for samples of $CaSO_4$:Tm.

In the dosimetric point of view, both materials present disadvantages and advantages. A good dosimetric peak should be a single peak (because it does not suffer interference from other peaks) at 200–300 °C [28]. This is a temperature range low enough to minimize the time and energy spent in the reading process, and high enough to minimize fading and IR emission of the equipment problems, granting thermal stability. $CaSO_4$:Tm,Ag presents a clear advantage of sensitivity, but its high temperature main peak appears only for heating rates below 4 °C/s. A clear disadvantage of this peak at elevated temperature

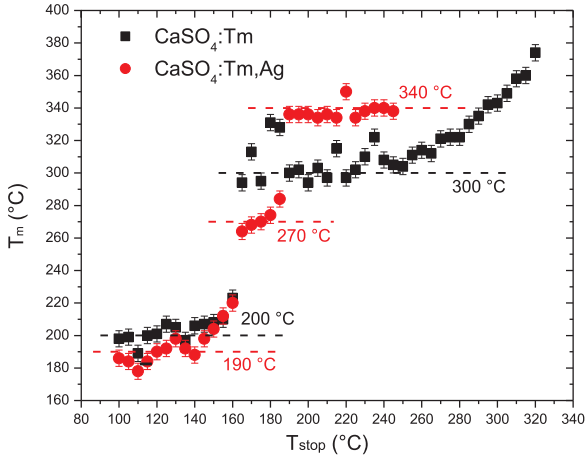

Fig. 9. T_m-T_{stop} curve of $CaSO_4$:Tm and $CaSO_4$:Tm,Ag samples obtained for various pre-heating temperatures (T_{stop}) after irradiation of 100 mGy ($^{90}Sr/^{90}Y$), evaluated at the heating rate of 10 °C/s. The pre-heating was performed in the Risö TL reader, before the reading.

is the intense infrared emission of the reader equipment at this temperature. Besides that, to reach higher temperatures, there must be higher energy expenditure, which results in a greater stress of the pellet. The $CaSO_4$:Tm samples present a good 300 °C dosimetric peak but, as can be demonstrated from Fig. 9, this peak is composed by an overlapping of several peaks in a broad temperature range. The complexity of TL curves, mainly the ones composed of many peaks, has been reported by some researchers [29,30]. This overlapping of several peaks also indicates the possibility of use of these composites as temperature indicators, as proposed by Doull et al. [30] for $CaSO_4$:Ce,Tb, by Souza et al. [31] for MgB_4O_7:Nd,Dy and by Junot et al. [15] for $CaSO_4$:Tb,Eu.

By means of the (T_m-T_{stop}) method it is also possible to determine the kinetic order of each peak of the TL glow curve of the materials. First-order kinetic peaks denote the predominance of the electron recombination process during the heating of the sample, while second-order kinetic peaks denote the predominance of the electron recapture process during the heating of the sample. For the samples of $CaSO_4$:Tm,Ag, the peaks at 190 °C and 270 °C, which show a slight rise in T_m as T_{stop} increases, can be evaluated as second-order peaks. The peak at 340 °C can be evaluated as a first-order peak, because it presents a plateau, that is, T_m remains constant as T_{stop} increases. For the samples of $CaSO_4$:Tm, the peak at 200 °C can be evaluated as a second-order peak and the peak at 300 °C seems to be composed of several peaks of indeterminated kinetic order.

Fig. 10 shows the OSL curves with an integration time of 40 s for the $CaSO_4$:Tm and $CaSO_4$:Tm,Ag samples, after an absorbed dose of 100 mGy from the $^{90}Sr/^{90}Y$ source. The results show that the composites present an intense signal, due to the high sensitivity of the samples, but do not exhibit a fast decay component, so that the OSL signal decays slowly and remains stored for a long time. This is not an expected behaviour for commercial OSL dosimeters since the OSL signal of such materials is characterized by a rapid exponential decay as long as the optically active traps are being emptied. So, it can be presumed that the traps responsible for the luminescent centers that give rise to the TL signal in these samples are not easily stimulated by blue LEDs. Kearfott et al. [6] reported that the most effective excitation wavelength for the Tm^{3+} primary emission at 455 nm is in the region of 355–370 nm, which is well distant from the 470 nm emission of the blue LEDs. The OSL sensitivity of such samples would probably be greater taking into account a proper selection of excitation source and detection equipment.

With the purpose to investigate the optical stimulation influence on the TL emission curve of the dosimeters and to verify the relationship

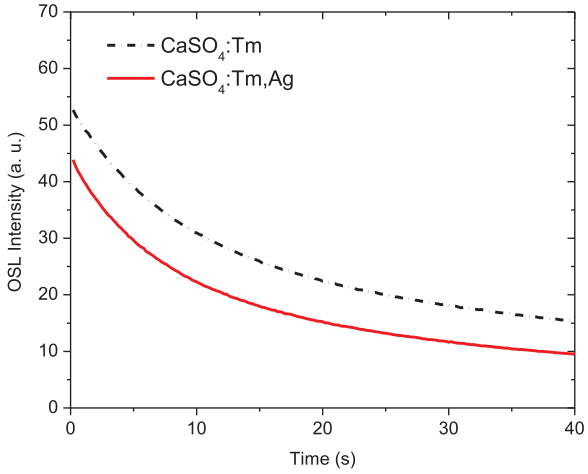

Fig. 10. OSL emission curves of $CaSO_4$:Tm and $CaSO_4$:Tm,Ag samples irradiated with 100 mGy ($^{90}Sr + ^{90}Y$).

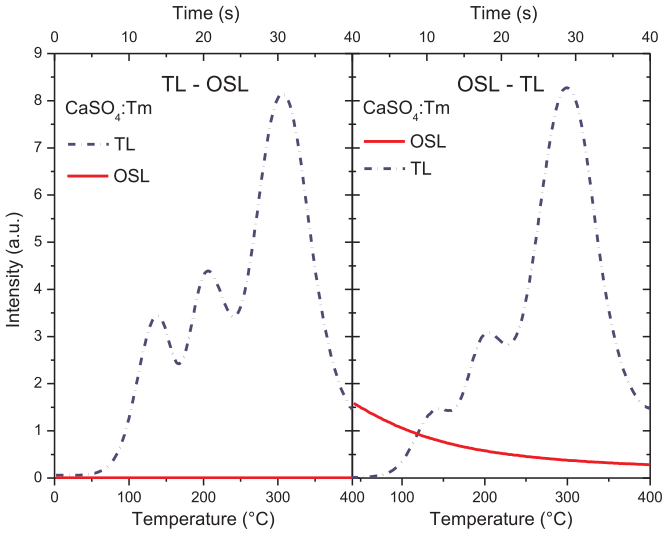

Fig. 11. TL-OSL and OSL-TL responses of the $CaSO_4$:Tm samples.

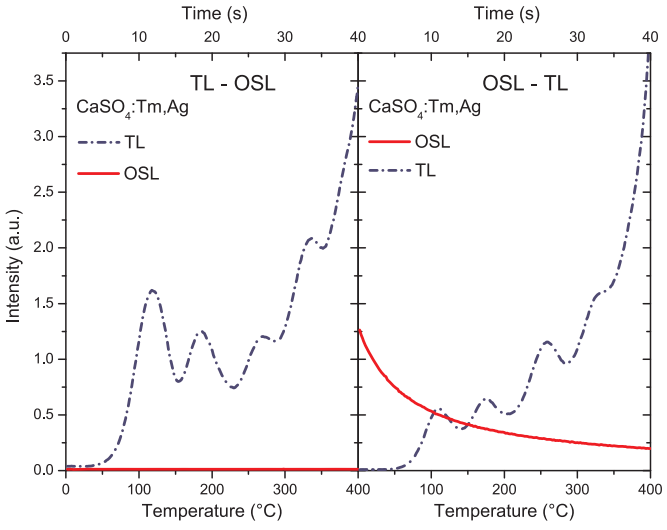

Fig. 12. TL-OSL and OSL-TL responses of the $CaSO_4$:Tm,Ag samples.

between the TL peaks and the OSL emission, consecutive TL → OSL and OSL → TL measurements were performed. The TL/OSL responses

obtained for the $CaSO_4$:Tm and the $CaSO_4$:Tm,Ag samples are shown in Figs. 11 and 12, respectively. As can be seen, the previous TL reading drastically reduces the OSL signal to background levels in both samples. This indicates that the optically active traps are easily emptied by thermal stimulation. However, the previous OSL reading slightly interferes in the following TL signal. From Fig. 11 it is easy to notice that the traps that give rise to the 145 °C and 200 °C peaks of the $CaSO_4$:Tm TL signal have a higher photoionization cross section than the traps that give rise to the 300 °C peak, once its TL intensity remains the same even after the optical stimulation. For the same photon flux of the light source, a higher photoionization cross section of the trap denotes a higher probability of release of the trapped electrons after an optical stimulation, which results in a more intense decay of the OSL signal [32]. For $CaSO_4$:Tm,Ag samples, it is possible to notice from Fig. 12 that only the traps that give rise to the 110 °C and 190 °C peaks have high photoionization cross sections for the 470 nm wavelength of the blue LEDs. This leads to conclude that the recombination centers responsible for the OSL emission are different from those responsible for the TL emission. Moreover, in these samples, the OSL emission is mostly due to shallow traps.

3.4. Reproducibility, linearity, minimum detectable dose and fading

Although all the pellets produced are identical, *i.e.* have the same form, dimensions and mass, due to the intrinsic sensitivity of each dosimeter, minor variations in response were observed among them. The ratio of the TL response of each dosimeter to the mean batch response of all dosimeters results in the dosimeter homogeneity coefficient (C_H). The ratio of the TL response of the dosimeter to the average response of the 5 reading cycles results in the dosimeter reproducibility coefficient (C_R). Table 1 shows the average values of the coefficients C_H and C_R of each studied material.

As observed in Fig. 13, all the TL responses were similar, with only a maximum deviation of 11% for $CaSO_4$:Tm samples. It can be observed that the TL response of $CaSO_4$:Tm,Ag samples slightly enhances after each irradiation-reading-annealing cycle. This fact may be caused by the deeper trapped charges, requiring a longer thermal treatment of the samples.

Thermoluminescent dosimeters shall preferentially present a linear relationship between the absorbed dose and the TL intensity. If the dose absorbed by the material is high enough for all capture charge centers to be filled, the material response saturates. To evaluate the dose-response curves of the samples, only 10 pellets with C_H and C_R below 5% were used. The dosimeters were irradiated with a dose range from 85 mGy to 3.5 Gy. A heating rate of 10 °C/s was used in the reader. Analyzing the dose-response curves with log axes in the same scale, as shown in Fig. 14, it can be observed that the TL response (integrated area of the whole curve) of the composites is linear in the applied dose range.

The lower detection limit or minimum detectable dose (D_0) of the materials produced was calculated by the Equation $\boldsymbol{D_0 = (\bar{B} + 3\sigma_{\bar{B}})f_c}$ proposed by Oberhofer e Scharmann [33], where $\boldsymbol{\bar{B}}$ is the average of the readings of 10 non-irradiated dosimeters; $\boldsymbol{\sigma_{\bar{B}}}$ is the standard deviation of the measures of non-irradiated dosimeters, and $\boldsymbol{f_c}$ is a calibration factor. The minimum detectable doses obtained for $CaSO_4$:Tm and $CaSO_4$:Tm,Ag samples were (8 ± 1) μGy and (6 ± 1) μGy, respectively, after irradiation with the $^{90}Sr/^{90}Y$ source. As can be seen, both samples presented very similar results, within the uncertainty.

Table 1
Medium homogeneity coefficient (C_H) and reproducibility coefficient (C_R) of produced samples.

Material	C_H (%)	C_R (%)
$CaSO_4$:Tm	7.8	7.1
$CaSO_4$:Tm,Ag	10.1	4.9

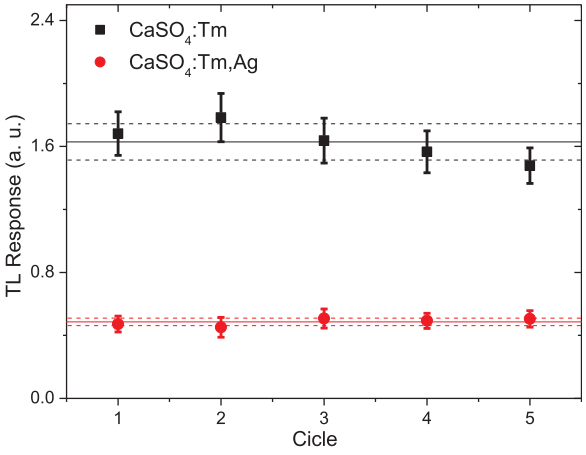

Fig. 13. TL response (integrated area of the whole curve) of $CaSO_4$:Tm and $CaSO_4$:Tm,Ag samples after each irradiation–reading–annealing cycle. The solid line represents the average TL response after 5 cicles. The dashed lines represent the average TL response ± standard deviation.

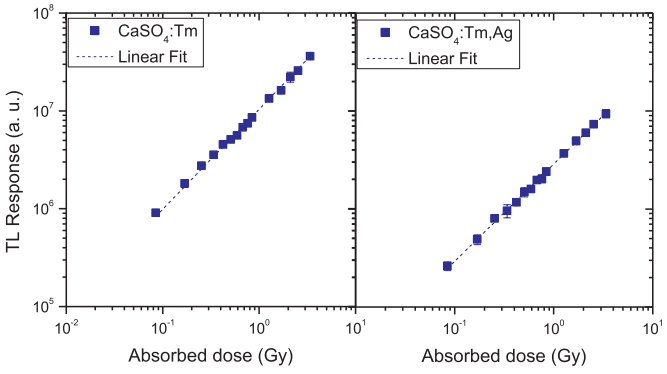

Fig. 14. TL response (integrated area of the whole curve) of $CaSO_4$:Tm and $CaSO_4$:Tm,Ag samples as a function of absorbed dose ($^{90}Sr/^{90}Y$).

Some parameters are crucial in maintaining the stability of the trapped charge carriers in the forbidden band gap of the crystal. The fading of a TL dosimeter should be as low as possible when these materials are stored under suitable conditions, such as room temperature and in low light. Fig. 15 presents the normalized TL responses of $CaSO_4$:Tm and $CaSO_4$:Tm,Ag samples after storage, showing the decay of the integrated area of the glow curves of the composites. In this normalization, the TL response of the samples just after the irradiation

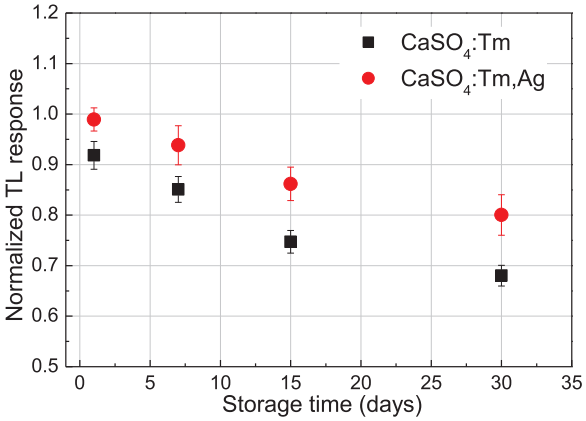

Fig. 15. Normalized TL response of $CaSO_4$:Tm and $CaSO_4$:Tm,Ag samples after irradiation with 1 Gy ($^{90}Sr + ^{90}Y$) and different storage time intervals.

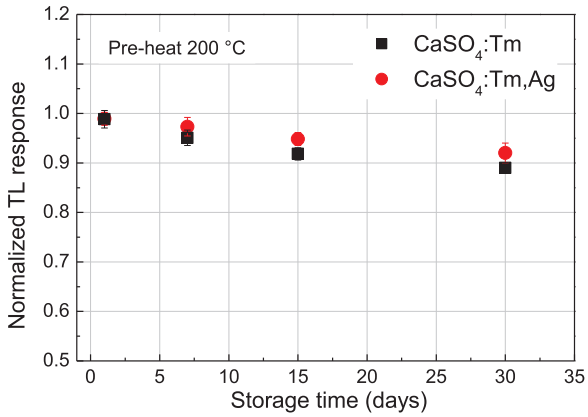

Fig. 16. Normalized TL response of $CaSO_4$:Tm and $CaSO_4$:Tm,Ag samples after a pre-heating of 200 °C for different storage time intervals and after irradiated with 1 Gy ($^{90}Sr + ^{90}Y$).

corresponds to a TL response of 1, and the TL response of the samples after storage time is shown as a percentage of the immediate TL response. It can be observed that the TL signal fading of the two composites is similar. The TL signal of $CaSO_4$:Tm samples decayed by 9% after one day, 15% after 7 days, 26% after 15 days, and 32% after one month. The $CaSO_4$:Tm,Ag samples exhibited a more satisfactory result, because their TL signal was reduced by approximately 14% over 15 days and 20% after one month.

The main negative feature of the dosimeters produced is the fading of the TL emission. While commercial dosimeters present a maximum fading of 5% per month, the composites of the present study exhibited fading four times faster. However, this can be minimized by evaluating the fading of the dosimeters after a reasonable pre-heating. Peaks at low temperatures usually exhibit low stability and decay much faster than peaks at higher temperatures corresponding to deeper traps. Fig. 16 presents the decay of the integrated area of the glow curves of the composites after a pre-heating at 200 °C. All samples presented low fading. After one month, the TL signal of $CaSO_4$:Tm and $CaSO_4$:Tm,Ag samples decayed by only 11% and 8%, respectively.

3.5. TL Emission spectrum

Fig. 17 shows the emission spectrum of the $CaSO_4$:Tm samples after an irradiation with a ^{60}Co source (100 Gy). The emissions of the Tm^{3+} ions, with the main emission at 455 nm ($^1D_2 \rightarrow {}^3F_4$), and less intense emissions at 348 nm ($^1D_2 \rightarrow {}^3H_6$), 355 nm ($^1D_2 \rightarrow {}^3H_6$), 482 nm ($^1G_4 \rightarrow {}^3H_6$) and 788 nm ($^3H_4 \rightarrow {}^3H_6$) can be observed. The same emissions were identified in the spectrum of the $CaSO_4$:Tm,Ag samples after an irradiation with a ^{60}Co source (100 Gy), as shown in Fig. 18. Both samples showed blue color during the heating process, consistent with the main emission at 455 nm. These spectra presented only divergences in the TL emission curves, as already explained. Therefore, the silver particles do not interfere in the emission spectrum of these samples, being only responsible for generating deeper capture centers, with higher activation energies, as discussed in Section 3.3. Madhusoodanan et al. [24] stated that the hole trap in the $CaSO_4$:Ag,Tm phosphor is characteristic of Ag^+ ion. Although Ag could be present in single or double valency, it is clear that it enters as Ag^+ in place of Ca^{2+} ion in the $CaSO_4$ lattice. Upon codoping with an Ag^+ ion, local charge compensation may occur when Tm^{3+} ion replaces the Ca^{2+} ion, and the Ca^{2+} vacancies would be removed. This occurs, in fact, since the insertion of Ag drastically reduces the intensity of the peak around 200 °C, characteristic of the sulfate radical related hole traps [24]. Thus, with the thermal stimulation, recombination of the holes released from Ag^+ ions may occur in electron traps and the recombination energy excites the Tm^{3+} ions. This results in a TL emission characteristic of

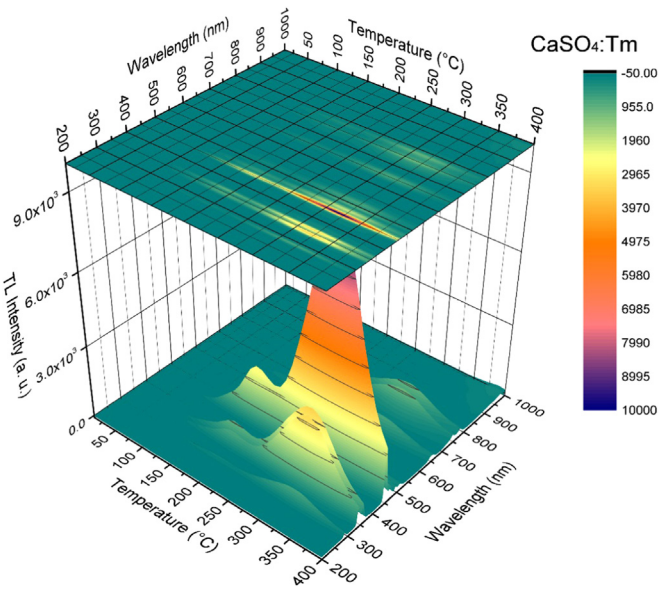

Fig. 17. Typical TL emission spectrum of a $CaSO_4$:Tm sample after irradiation with 100 Gy (^{60}Co).

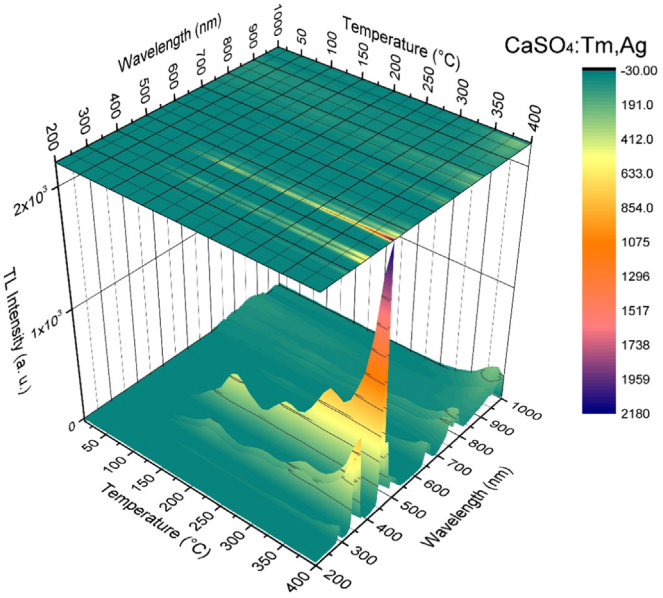

Fig. 18. Typical TL emission spectrum of a $CaSO_4$:Tm,Ag sample after irradiation with 100 Gy (^{60}Co).

Tm^{3+} as observed in the emission spectra. Furthermore, the low luminescent intensity presented by the $CaSO_4$:Tm,Ag samples in the photoluminescence spectrum can be explained by the high energy of activation of the recombination centers present in these samples. From the dosimetric point of view, this displacement of the peak to temperatures above 350 °C makes it disadvantageous for use in radiation dosimetry. It should be very interesting to verify the influence of the concentration of the silver particles in the displacement of the peak Figs. 17 and 18.

4. Conclusions

The production route used in the crystal growth was simple and viable. Samples produced exhibited only a single phase corresponding to the crystal structure of anhydrite. The optical characterization evidences that the optical band gap of these samples is around 6.7 eV,

corresponding to the first excitation band. The $CaSO_4$:Tm samples showed TL emission glow curves with peaks in temperatures proper for dosimetry. The $CaSO_4$:Tm,Ag samples presented a very intense peak displaced to high temperatures, which is not adequate for dosimetry, and only observed by applying heating rates below 4 °C/s. The OSL signal of the samples was intense, but do not present a fast decay component after stimulation with blue LEDs. The TL signal fading of the samples was reasonably satisfactory after a pre-heating of 200 °C, and may be taken into account with an appropriate correction factor. The TL emission spectra confirmed the incorporation of the Tm^{3+} ion into the calcium sulfate matrix. The $CaSO_4$:Tm and $CaSO_4$:Tm,Ag materials presented some TL properties appropriated for dosimetric purposes, such as linearity, reproducibility and minimum detectable dose in the order of micrograys. All these characteristics evidence the applicability potential of the studied samples as luminescent dosimeters. The glow curves results also indicate the possibility of use of these composites as temperature indicators.

Acknowledgments

The authors thank the Brazilian Agencies CNEN, CNPq (grants 150678/2017-7 and 301335/2016-8), CAPES and MCTIC for their partial financial support. They are also grateful to the Brazilian Syncrotron Light Laboratory and the TGM beamline staff for their valuable help on the measurements taken under the TGM#20180009 Internal Research proposal.

References

[1] A.R. Lakshmanan, Photoluminescence and thermostimulated luminescence processes in rare-earth-doped CaSO4 phosphors, Prog. Mater. Sci. 44 (1999) 1–187.
[2] E.G. Yukihara, S.W.S. McKeever, Optically Stimulated Luminescence: fundamentals and Applications, John Wiley & Sons Ltd, Oklahoma, 2011.
[3] U. Madhusoodanan, M.T. Jose, A. Tomita, A.R. Lakshmanan, New thermostimulated luminescence phosphors based on $CaSO_4$:Ag,RE, J. Lumin. 87–89 (2000) (1300–1032).
[4] M.S. Kulkarni, R.R. Patil, A. Patle, N.S. Rawat, P. Ratna, B.C. Bhatt, S.V. Moharil, Optically stimulated luminescence from $CaSO_4$:Eu - Preliminary results, Radiat. Meas. 71 (2014) 95–98.
[5] V. Guckan, V. Altunal, N. Nur, T. Depci, A. Ozdemir, K. Kurt, Y. Yu, I. Yegingil, Z. Yegingil, Studying $CaSO_4$:Eu as an OSL phosphor, Nucl. Instrum. Methods Phys. Res. B 407 (2017) 145–154.
[6] K.J. Kearfott, W.G. West, M. Rafique, The optically stimulated luminescence (OSL) properties of LiF:Mg,Ti, $Li_2B_4O_7$:Cu, $CaSO_4$:Tm, and CaF_2:Mn thermoluminescent (TL) materials, Appl. Radiat. Isot. 99 (2015) 155–161.
[7] K.R.E. Saraee, A.A. Kharieky, M. Khosravi, M.R. Abdi, H.Z. Zeinali, Themoluminescence properties of nanocrystalline of $BaSO_4$:Dy,Tb irradiated with gamma rays, J. Lumin. 137 (2013) 230–236.
[8] M. Kumar, S.K. Gupta, R.M. Kadam, Near white light emitting $ZnAl_2O_4:Dy^{3+}$ nanocrystals: sol–gel synthesis and luminescence studies, Mater. Res. Bull. 74 (2016) 182–187.
[9] U. Madhusoodanan, M.T. Jose, R. Indira, T.K. Gundo Rao, Luminescence studies in $KMgF_3$:Eu,Ag, Indian J. Pure Appl. Phys. 47 (2009) 459–460.
[10] M. Zahedifar, N. Taghavinia, M. Aminpour, Synthesis and thermoluminescence of ZnS:Mn^{2+} nanoparticles, AIP Conf. Proc. 929 (2007) 128–132.
[11] Yashaswini, C. Pandurangappa, N. Dhananjaya, M.V. Murugendrappa, Photoluminescence, Raman and conductivity studies of CaSO4 nanoparticles, Int. J. Nanotechnol. 14 (2017) 845–858.
[12] D.O. Junot, D.F. Vasconcelos, M.A.P. Chagas, M.A. Couto dos Santos, L.V.E. Caldas, D.N. Souza, Silver addition in $CaSO_4$:Eu, TL and TSEE properties, Radiat. Meas. 46 (2011) 1500–1502.
[13] D.O. Junot, M.A. Couto dos Santos, P.L. Antonio, L.V.E. Caldas, D.N. Souza, Feasibility study of $CaSO_4$:Eu, $CaSO_4$:Eu,Ag and $CaSO_4$:Eu,Ag(NP) as thermoluminescent dosimeters, Radiat. Meas. 71 (2014) 99–103.
[14] D.O. Junot, J.J. Rodrigues Jr, D.N. Souza, M.A. Couto dos Santos, L.A.O. Nunes, The $CaSO_4$:Eu-Ag composite material: thermo-photoluminescence study, Radiat. Meas. 70 (2014) 1–4.
[15] D.O. Junot, J.P. Barros, L.V.E. Caldas, D.N. Souza, Thermoluminescent analysis of $CaSO_4$:Tb,Eu crystal powder for dosimetric purposes, Radiat. Meas. 90 (2016) 228–232.
[16] E. Ekdal, J. Garcia Guinea, A. Kelemen, M. Ayvacikli, A. Canimoglu, A. Jorge, T. Karali, N. Can, Cathodoluminescence and Raman characteristics of $CaSO_4:Tm^{3+}$, Cu phosphor, J. Lumin. 161 (2015) 358–362.
[17] M.A.P. Chagas, M.G. Nunes, L.L. Campos, D.N. Souza, TL properties of anhydrous $CaSO_4$:Tm improvement, Radiat. Meas. 45 (2010) 550–552.
[18] R.L. Cavasso Filho, A.F. Lago, M.G.P. Homem, S. Pilling, A. Naves de Brito, Delivering high-purity vacuum ultraviolet photons at the Brazilian toroidal grating monochromator (TGM) beamline, J. Electron Spectrosc. Relat. Phenom. 156–158 (2007) 168–171.
[19] T. Karali, A.P. Rowlands, P.D. Townsend, M. Prokic, J. Olivares, Spectral comparison of Dy, Tm and Dy/Tm in thermoluminescent dosimeters, J. Phys. D: Appl. Phys. 31 (1998) 754–765.
[20] I. Kudryavtseva, M. Klopov, A. Lushchik, Ch Lushchik, A. Maaroos, A. Pishtshev, Electronic excitations and self-trapping of electrons and holes in $CaSO_4$, Phys. Scr. 89 (2014) 044013.
[21] M. Zahedifar, M. Mehrabi, S. Harooni, Synthesis of $CaSO_4$:Mn nanosheets with high thermoluminescence sensitivity, Appl. Radiat. Isot. 69 (2011) 1002–1006.
[22] Z. Hu, C. Zhang, Y. Li, B. Ao, First-principles study of structural, electronic, optical and bonding properties of celestine, $SrSO_4$, Solid State Commun. 158 (2013) 5–8.
[23] R.A.P.O. D'Amorim, M.I. Teixeira, L.V.E. Caldas, S.O. Souza, Physical, morphological and dosimetric characterization of the Teflon agglutinator to thermoluminescent dosimetry, J. Lumin. 136 (2013) 186–190.
[24] U. Madhusoodanan, M.T. Jose, A. Tomita, W. Hoffmann, A.R. Lakshmanan, A new thermostimulated luminescence phosphor based on $CaSO_4$:Ag,Tm for applications in radiation dosimetry, J. Lumin. 82 (1999) 221–232.
[25] M.A. Melo Jr., L.S.S. Santos, M.C. Gonçalves, A.F. Nogueira, Preparation of silver and gold nanoparticles: a simple method to introduce nanotechnology into teaching laboratories, Quim. Nova. 35 (2012) 1872–1878.
[26] N. Salah, Thermoluminesence of gamma rays irradiated $CaSO_4$ nanorods doped with different elements, Radiat. Phys. Chem. 106 (2015) 40–45.
[27] C. Furetta, Questions and Answers on Thermoluminescence (TL) and Optically Stimulated Luminescence (OSL), World Scientific Publishing, London, 2008.
[28] S.W.S. McKeever, M. Moscovitch, P.D. Townsend, Thermoluminescent Dosimetry Materials: Properties and Uses, Nuclear Technology Publishing, Ashford, 1995.
[29] M.G. Nunes, L.L. Campos, Study of $CaSO_4$:Dy and LiF:Mg,Ti detectors TL response to electron radiation using a SW solid water phantom, Radiat. Meas. 43 (2008) 459–462.
[30] B.A. Doull, L.C. Oliveira, D.Y. Wang, E.D. Milliken, E.G. Yukihara, Thermoluminescent properties of lithium borate, magnesium borate and calcium sulfate developed for temperature sensing, J. Lumin. 146 (2014) 408–417.
[31] L.F. Souza, P.L. Antonio, L.V.E. Caldas, D.N. Souza, Neodymium as a magnesium tetraborate matrix dopant and its applicability in dosimetry and as a temperature sensor, Nucl. Instrum. Methods A 784 (2015) 9–13.
[32] J.V.B. Valença, A.C.A. Silva, N.O. Dantas, L.V.E. Caldas, F. d'Errico, S.O. Souza, Optically stimulated luminescence of the $20Li_2CO_3 – (X)K_2CO_3 – (80 - X)B_2O_3$ glass system, J. Lumin. 200 (2018) 248–253.
[33] M. Oberhofer, A. Scharmann, Applied Thermoluminescence Dosimetry, CRC Press, Ispra, 1981.